ASEAN Engineering Journal

Full Paper

EXPERIMENTAL AND NUMERICAL ANALYSIS ON THE LOCALIZED STRESS-STRAIN BEHAVIOR OF HOLLOW CONCRETE MASONRY WALLS

Kabiru A. Musa, MZAM Zahid, B.H. Abu Bakar

School of Civil Engineering, Tuanku Syed Sirajuddin Engineering Campus, Universiti Sains Malaysia, 14300 Nibong Tebal, Penang, Malaysia.

Article history
Received
07 August 2025
Received in revised form
01 October 2025
Accepted
01 November 2025
Published online
31 May 2026

*Corresponding author
ayagi@student.usm.my

Graphical abstract

Loading Frame

Abstract

This study examines the experimental and numerical analysis of the stress-strain behavior of full-scale hollow concrete block (HCB) masonry walls under axial compressive loading, considering the influence of different boundary conditions. Four wall panels were constructed using standardized HCB and bond beam blocks (BBB), with consistent dimensions and mortar compositions. Following a 28-day curing period, the panels were subjected to gradually increasing axial loads under four distinct boundary configurations: fixed–fixed, fixed–free, fixed–pinned, and pinned–pinned. The investigation aims to assess how these boundary conditions affect the structural performance and failure characteristics of HCB wall systems. Key parameters, including lateral deflection, axial displacement, and crack formation, were measured using LVDTs and a data logging system. Results indicate that boundary conditions significantly affect the deformation and failure behavior of the walls. The highest failure load (504 kN) was observed in the panel with fixed-fixed supports, while the lowest (342 kN) occurred in the fixed-free configuration. Cracking initiated in vertical mortar joints and progressed through bed joints and HCB units, with failure primarily governed by mortar degradation. The findings highlight the importance of support conditions in evaluating the structural performance of HCB walls and offer valuable data for improving design practices.

Keywords: Concrete hollow block; stress-strain, axial compression; numerical; experiment

1.0 INTRODUCTION

Masonry, is one of the oldest known building materials, has been used for centuries by various civilizations due to its accessibility, aesthetic appeal, functional versatility, and cost-effectiveness [1], [2], [3]. It remains prevalent in contemporary construction [4], [5], [6] and continues to be the subject of extensive research. Many investigations have evaluated how masonry walls behave under axial loads, examining parameters such as block type, slenderness ratio, and load eccentricity. However, there is a paucity of experimental data specifically on hollow concrete block (HCB) walls under direct compressive loading.

For example, Zhou et al. [7] studied the stress-strain response using HCB of various strengths and mortar specimens under uniform boundary conditions. Keshava and Raghunath [8] assessed the impact of axial loading and eccentricity on the load capacity of both solid and hollow block walls. Amalkar et al. [9] tested nine cellular HCB walls to observe the effects of slenderness and eccentric loading, five under double-ended eccentricity and four under pure axial load. Recently, Dharek et al. [10] conducted similar axial compression tests on HCB walls. These studies report significant variability, especially with higher-strength blocks and more slender walls, all under cantilever boundary conditions (fixed-fixed, fixed-free).

Edge restraints in laboratory tests are crucial, as they limit movement and rotation, directly influencing crack initiation and

failure mode [11]. Under axial compression, slender HCB panels typically act as one-way elements, bending uniaxially with vertical supports and a free edge [12]. Although some research has explored two-way boundary conditions for HCB walls [13], [14], [15], few experimental and numerical studies address one-way supports [16]. Moreover, the roles of panel aspect ratio, loading type, and boundary conditions are not fully understood. Thus, comprehensive full-scale experiments are needed to clarify how these factors govern failure mechanisms and overall behavior under axial loads.

Numerical modeling of masonry can be conducted using either macro- or micro-modelling approaches, with the choice depending on the desired level of accuracy and computational efficiency [17]. Micro-modelling has proven to be a highly effective technique for simulating masonry behavior under various loads and support conditions. While it is commonly used to model the in-plane response of both reinforced and unreinforced masonry walls, its application in studying axial load behavior remains limited. Given its advantages such as lower computational demand and easier mesh generation, this study employs a micro-modelling approach [17].

2.0 METHODOLOGY

2.1 Block Testing

The HCB units utilized in this investigation were produced in a single production batch and had nominal dimensions of 190 mm × 140 mm × 390 mm. They were purchased from the same manufacturer. The prepared HCBs: (a) HCB and (b) bond beam block (BBB) is shown in Figure 1. The BBB (called a U-block) is made up of specialized blocks that are filled with grout to hold a reinforced bar in place [18], [19]. The dimensions and specifications of the BBBs were the same as the HCB units.

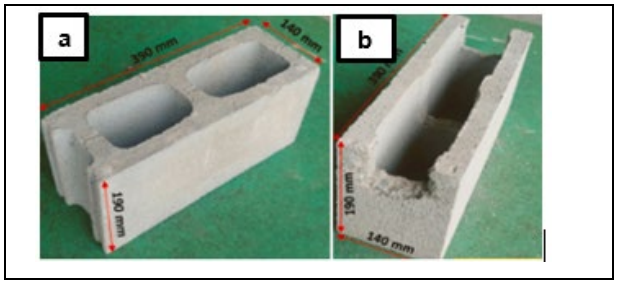

Figure 1 Prepared Masonry blocks: (a) hollow concrete block and (b) bond beam block

HCB units were subjected to compressive strength testing to guarantee that they satisfied the applicable unit specification's minimum strength requirements [20]. An axial compressive load was applied to the HCB units at a loading rate of 0.25 N/mm^2/s with a maximum capacity of 1000 kN until failure.

2.2 Wall Construction And Axial Compressive Test

Four full-scale wall panels (named C1, C2, C3, and C4) used in the investigation were evaluated with an axial force that was uniformly distributed. These panels had a height/length ratio of 1:16 (990 × 1590 mm) and a slenderness ratio of 1:11 (height/thickness). The mortar bed had a thickness of roughly 10 mm. A competent mason worked under supervision to construct the wall panels, which used a running bond pattern. The lowermost layer of the wall panels was positioned in a thick layer of mortar on a suitably sized and shaped steel plate to facilitate the safe transportation and installation of the panel walls onto the test rig. At the final course of the wall panels, BBB units that had the same proportions as the HCB units were employed. Concrete and reinforcement were only added to the cells where BBB units were present. The same strengthening plan was used in the BBB units for every wall panel: Four prefabricated ϕ12 mm steel bars with welded steps at every 300 mm. After fabrication, the panels were covered with polyethylene sheet for three days. After that, they were left exposed and allowed to air cure in a laboratory setting (temperature between 27 °C to 30 °C) for at least 28 days until testing.

A load cell was attached to a hydraulic jack to quantify the applied compression load. A Linear Variable Differential Transformer (LVDT 1), installed at the top of the wall, was used to measure the vertical displacement. Furthermore, LVDT 2 was used to detect lateral deformation. It was positioned strategically at the middle of the walls' compression face, as shown in Figure 2. The height lateral deflection curve was then plotted along the vertical centreline of the block wall panels using the collected readings by dividing the difference in the wall's height as measured by the LVDTs by the initial height, the strain was calculated. The LVDTs were linked to a multi-channel data logger, which logged the readings and made the data collection easier following ASTM E7-15 [21] recommendations.

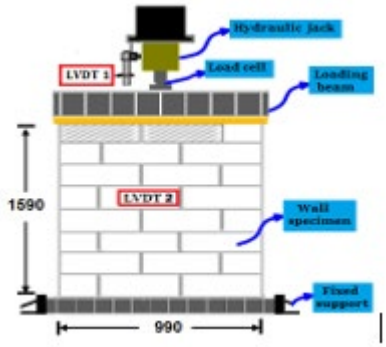

Figure 2. Schematic representation of tested walls

As seen in Figure 3, the loading frame with an 1800 kN load capacity was fastened to the laboratory floor. The boundary conditions C1 (fixed-fixed), C2 (fixed-free), C3 (fixed-pinned), and C4 (pinned-pinned) were assigned. During mechanical testing, boundary conditions were configured according to their supports. Fixed- fixed support was clamped at both ends of the specimen to prevent translation and rotation in all directions. Fixed- free support was clamped at one end of the specimen to prevent translation and rotation in all direction leaving the other end completely unconstrained, allowing it to move or rotate freely. Fixed- pinned support was clamped at one end of the specimen to prevent translation and rotation in all direction, while pin support was used at the other end, allowing rotation but preventing translation in any direction. Pinned- pinned support used pin supports at both ends allowing rotation but preventing translation in any direction. The axial load was

incrementally applied to the panels until the panels experienced failure. The loading process was gradual, and the rate of loading was maintained at approximately 50 kN/min to allow stress distribution and to monitor the cracks in the specimens. Failure was determined to have occurred when the load drops by 25%, indicates that the specimen has lost a significant portion of its load- bearing capacity. Throughout the course of the tests, careful attention was paid to the force values, and the locations where cracks emerged were meticulously observed and systematically recorded.

Figure 3 Boundary condition and loading frame for wall panels

2.3 Numerical Modeling

Computer-aided design (CAD) models of the HCB walls were developed and analyzed using ANSYS Design of Experiments (DOE) and optimization tools. Engineers used modelling idealization because it creates effective and efficient models that provide valuable insights into complex system. Element discretization enable numerical computation of the solution by converting continuous equations into discreate algebraic equation. It creates a mesh that accurately represents the geometry and captures the relevant physics. The axial compression behavior of the HCB wall panels was simulated using ANSYS 2021 R1 through micro-modeling techniques. In the numerical model, the HCB wall was treated as an isotropic material with uniform properties and distributed cracks. The properties of materials can be both measured or calibration, depending on the specific requirements and available data. Material properties can be isotropic, anisotropic, linear or non-linear, depending on the material's behavior. Previous research has employed the smeared crack method combined with finite element analysis to predict the performance of unreinforced masonry, showing strong agreement with experimental findings [22], [23], [24]. The ANSYS simulations were used to assess strength, displacement, and stress distribution. According to E. V. Caburmay et al. [25] the use of finite element (FEA) software has been beneficial in evaluating the stresses, deformations and strains. These results were compared to those obtained from physical testing to evaluate the accuracy and reliability of the software. Outputs from ANSYS could be presented in both tabular and graphical formats [26]. Due to its capability to handle complex geometries and mathematical models, ANSYS proves to be an effective tool for simulating block masonry structures.

ANSYS software was used to perform a numerical analysis of masonry buildings [27], and ANSYS software was used to create the first masonry building in the context of numerical simulation and a macro-modeling technique [28], [29]. For numerical modelling and nonlinear analysis of unstrengthened and reinforced masonry walls, the commercial software ANSYS v.15 was used [12]. Prism tests were performed using ANSYS14 to determine the compressive strength of masonry [30]. FE software and the general-purpose finite element method were used to investigate the in-plane behaviour of brick masonry wall panels using ANSYS 6.0 simulation software [31]. The numerical results agreed with the experimental load-deflection plots and cracking patterns when commercial software ANSYS was used to create a FE micromodel for block walls that were tested under vertical compression and in-plane cyclic shear loading [32].

3.0 RESULTS AND DISCUSSION

The HCB unit used in the study has water absorption roughly 7.362% and has a density of about 1,203 kg/m3. For the mortar type II, designated 1:3, which had a consistency of roughly 10 ± 1 mm, the dropping ball test was employed. Cubic molds of 50 mm by 50 mm by 50 mm were used to cast the mortar and grout ASTM C-109/ C109M [33] and were put to the test on the day the walls were tested. After the cubes were removed and cured in water at 20°C for 28 days, they were first kept and covered with a polythene sheet for 24 hours. To find the mortar's relative density, the cubes were weighed in both air and water. The compressive strength of the mortar was then measured by loading them at a rate of 0.1N/mm^2/sec. Table 1 displays the outcomes of the HCB's workability, water absorption, and density tests as well as the strength characteristics of the HCB and mortar.

Table 1 Engineering properties of Hollow concrete block

Engineering Properties	Values (Unit)
Workability (dropping ball apparatus)	10 ± 1mm
Water absorption	7.362%
Density	1,203 kg/m3
Compressive Strength (HCB unit)	8.39 N/mm2
Compressive strength (mortar)	21.34 MPa
Tensile strength (mortar)	13.23 MPa
Flexural Strength (HCB unit)	3.91 N/mm2

The maximum axial displacement and lateral deflection of panels C1–C4 as well as the test results are summarized in Tables 2. The idea is to show their average behaviour and amount of

displacement when loaded. The average reading was obtained from the data logger of the transducer's attachment to the HCB wall panels. Axial load versus lateral deflection is a relationship that describes the HCB wall panels' structural deformation response to loading and load versus lateral displacement profiles for a wall, because failure occurs primarily at the block-to-mortar interface. Both models can accurately predict the load versus axial displacement relationship for the wall panel C1-C4. Peaks in the post-cracking behaviour indicated that the cracking caused new cracks to form and stress to be redistributed in the wall panels, and when the blocks were assumed to be elastoplast, no such behaviour was observed. The primary cause of failure was the mortar joints, not the HCB units.

Table 2 Summary of the maximum axial displacements and lateral deflections for wall panels C1-C4

Wall panels	Boundary Condition		Loading arrang.	Failure load (kN)
	Bottom	Top		
C1	Fixed	Fixed	UDL	504
C2	Fixed	Free	UDL	342
C3	Fixed	Pinned	UDL	502
C4	Pinned	Pinned	UDL	406
Wall panels	Cracking load (kN)	Max. axial displacement (mm)	Maximum lateral deflection (mm)	
C1	320	24.07	18.53	
C2	250	26.07	27.36	
C3	300	19.72	18.96	
C4	300	20.85	25.95	

Figure 4 presents axial displacement versus lateral deflection (a and b), revealing an almost linear relationship up to approximately two-thirds of the ultimate load, followed by a nonlinear response. This early-stage behavior, described as nonlinear progressive stiffening, is attributed to initial specimen settlement and the crushing of mortar joints and voids. Among the panels, C2 (with fixed-free boundary conditions) showed the highest strain concentration. As summarized in Table 2, the small variation in the maximum axial displacement and lateral deflection across the panels indicates structural stability. This suggests that buckling did not occur in any of the tested specimens and can thus be considered negligible.

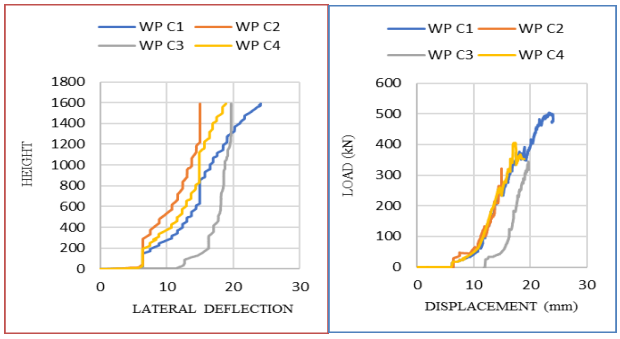

Figure 4 Lateral deflection and axial displacement of the wall panels

3.1 Numerical Analysis

Figure 5 presents the structural deformation result of wall panels C1-C4. Maximum Principal Elastic Stress (MPES) refers to the normal stress acting along the principal plane of a structural element, this is the axial stress developed to resist deformation. The Maximum Principal Elastic Strain (MPEST) represents the maximum and minimum normal strain values [34]. On the other hand, Equivalent Elastic Stress (EES) relates to the internal resistance that remains in a body once it returns to its original shape and size after deformation. According to Elamin & Lei (2020) [35] stress concentrations in elastic materials can cause localized failures and, kink bands may form and propagate rapidly, leading to total strength loss. Equivalent Elastic Strain (EEST) is the strain that fully recovers once the load is removed [36].

To achieve an accurate result, CHB block wall panels C1-C4 were finey meshed, and micro-modelling was used. A compressive load was applied at the top as pressure loading. Loading was applied in stages, and the bottom surface of the wall panel was constrained. Mesh refinement studies are commonly performed in computational simulations, particularly in finite element analysis (FEA) and computational fluid dynamic (CFD). This is to ensure accuracy, to verify the solution converges to a consistent result as the mesh is refined. The study is also an essential part of the simulation workflow, ensuring that computational models provide reliable and accurate predictions. According to [37] In the field of computational mechanics, mesh refinement is essential for achieving high-fidelity solutions in finite element method (FEM) simulations.

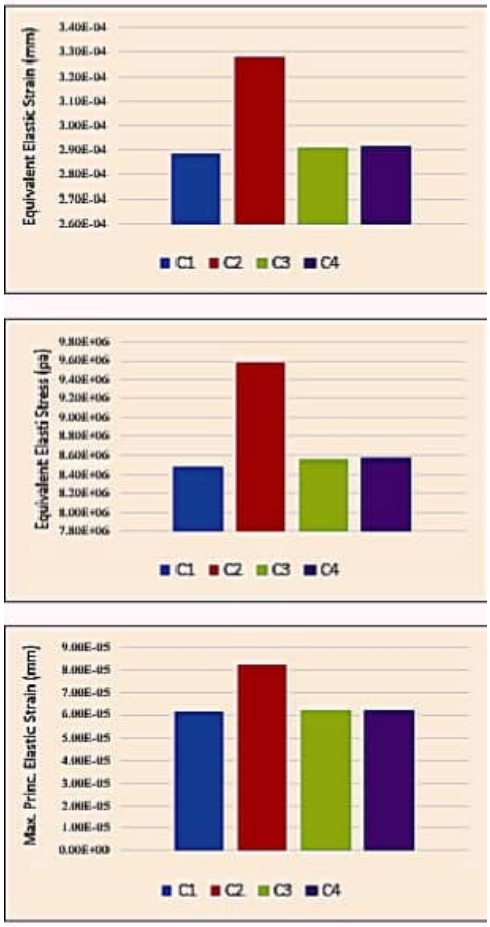

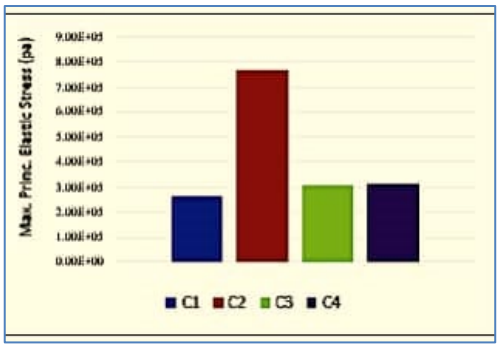

Figure 5 Structural deformation of wall panels C1-C4

3.2 Failure Modes

Figure 6 represents the failure modes observed in the tested walls. Initially, all crack patterns from wall panels C1-C4 were primarily vertical splitting caused by horizontal tensile stress present in the HCB units, the cracks run parallel to the loading axis through the centre of the wall panels. The mode of cracking was like that observed in the studies by Fundi et al., 2018 [37] and T. EL-Salakawy and G. Hamdy, 2021 [29]. According to their studies, the first vertical crack appeared in the middle of a solid wall panel at a vertical load of 160kN and more vertical cracks appeared as the load increased until failure occurred. In the present study, the first cracks in the wall panels were observed in the spandrel area's head joints, and the cracks caused by vertical loads then propagated to the middle of the wall at 250, 300, 300, and 320 kN. Average failure loads were 504, 502, 342, and 406 kN for C1–C4, respectively. Two critical failure mechanisms are: (a) interface debonding, and (b) pore collapse in the mortar. A combination of mortar crushing, and unit tension failure governed the panels' ultimate strength.

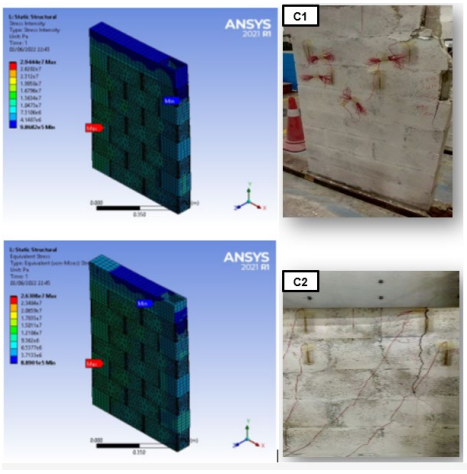

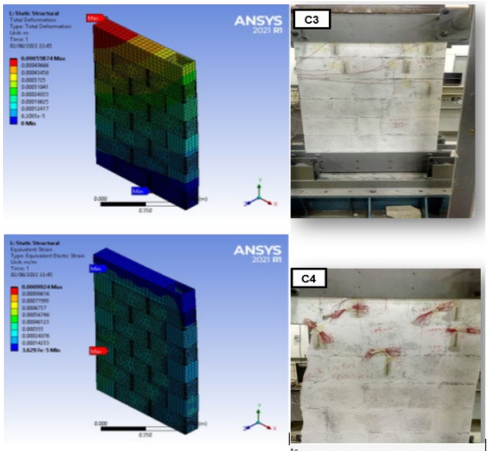

Figure 6 Failure for wall panels C1-C4

3.2 Comparison and Discussion Of Results

Figure 7 presents the stress-strain curves derived from both experimental and numerical analyses, showing close alignment in ultimate compressive strength values. The results indicate a strong correlation between applied stress and the observed failure mechanisms. The stress-strain behavior of the masonry elements was characterized by an initial nonlinear response, followed by a linear phase, and then a transition to nonlinear softening approaching peak load. This behavior reflects a phenomenon known as nonlinear progressive stiffening, which is attributed to initial specimen settlement and the crushing of interstitial voids at the onset of compressive loading. Two primary failure modes were identified in assessing the cohesive strength of HCB wall panels: (a) loss of adhesion at the material interfaces, and (b) structural collapse due to pore compression within the mortar matrix. Experimental results demonstrated that cracking initiates in the mortar joints, progressing under load and ultimately leading to failure. This is due to the high porosity of mortar and its tendency to shrink as voids are filled, creating weak paste-aggregate interfaces prone to cracking.

In the numerical analysis, the model behaves as a homogeneous material, leading to a uniform load dispersion at approximately 45°. In contrast, actual masonry is a composite system of blocks and mortar, and the load distribution does not follow the same uniform pattern. Mortar joints, typically weaker than the blocks, are often the first to fail, reducing the overall compressive strength of the masonry. Although the numerical model simplifies the wall as a monolithic material, idealizing it as a composite wall yield a more accurate representation of physical behavior.

The comparison between experimental and numerical results revealed that the experiment determined compressive strength was approximately 50% higher than the strength predicted by ANSYS simulations. Consequently, it is recommended that a correction factor of 1.5 be applied to ANSYS-derived compressive strength values to better reflect actual performance. While experimental observations captured a more complex failure process including both mortar crushing and tensile rupture of the blocks, the numerical simulations were unable to fully replicate these behaviors, particularly in terms of accurately predicting the failure load. This underscores

the limitations of current modeling approaches in capturing the intricacies of masonry failure.

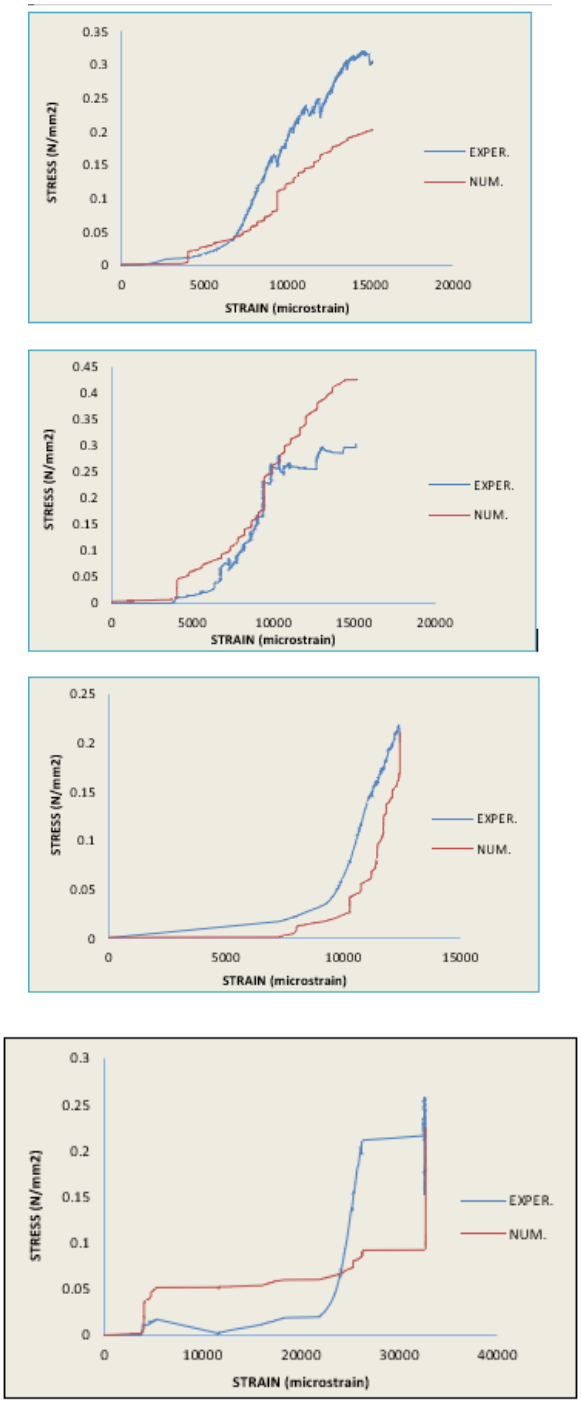

Figure 7 Stress-Strain Behavior Of HCB Experimentally And Numerically

4.0 CONCLUSION

This study presented both experimental and numerical investigations into the localized stress-strain behavior of hollow concrete block (HCB) wall panels. Four full-scale wall panels were designed and tested under distributed axial loading. The corresponding load and displacement data were analyzed in detail. The peak loads for panels C1–C4 were 504, 502, 342, and 406 kN, respectively. The numerical results obtained using ANSYS closely matched the experimental outcomes.

Key conclusions drawn from this study are as follows:

a) The experimental and numerical approaches effectively examined localized stress-strain responses in HCB wall panels. The data gathered offers valuable insights for the structural design and evaluation of axially loaded HCB walls under varying boundary conditions.

b) It is found that the axial load-deflection behavior of HCB wall shows linear responses in the initial loading region, which followed by nonlinear response up to ultimate failure load.

c) The development and progression of cracks were largely influenced by the mortar, which played a significant role in the failure of the wall panels. The discrepancy in behavior between the mortar and block units was a critical factor in crack initiation.

d) Analysis indicated that when the base was fully restrained while the top edge was left free (fixed-free support) must of the time affect the wall panel by receiving more stress-strain concentration

Acknowledgement

The authors express their gratitude to the School of Civil Engineering at Universiti Sains Malaysia (USM) for providing financial support.

Conflicts of Interest

The author(s) declare(s) that there is no conflict of interest regarding the publication of this paper

References

[1] A. S. M. Akid, M. H. Rashid, and M. H. Rahman Sobuz, 2021, "Effect of masonry infill wall with opening on reinforced concrete frame due to seismic loading: Parametric study," *International Journal of Structural Engineering.* 11(1): 84–105, DOI: 10.1504/IJSTRUCTE.2021.112103.

[2] Z. Liu et al. 2019, "Investıgatıon of usıng ansys software ın the determınatıon of stress behavıours of masonry walls under out of plane cyclıng load," *International Journal of Physical Sciences* 5(2): 97–108. DOI: 10.17577/ijertv4is070814.

[3] K. A. Musa, B. H. A. Bakar, and U. J. Udi, 2023, "Influence of Opening and Boundary Conditions on the Behavior of Concrete Hollow Block Walls: Experimental Results," *Journal of Engineering and Technological Sciences.* 55(5): 569–576, DOI: 10.5614/J.ENG.TECHNOL.SCI.2023.55.5.6.

[4] X. Yang, H. Wu, J. Zhang, and H. Wang, 2019, "Shear Behavior of Hollow Concrete Block Masonry with Precast Concrete Anti-Shear Blocks," *Advances in Materials Science and Engineering* DOI: 10.1155/2019/9657617.(Please don't use short form)

[5] M. Umair, M. Alam, and S. M. Anas, 2022, "Experimental studies on blast performance of unreinforced masonry walls of clay bricks and concrete blocks: a state-of-the-art review," *International Journal of Masonry Research and Innovation (IJMRI)* 1(1): 1, DOI: 10.1504/ijmri.2022.10049719.(Please don't use short form)

[6] I. E. Edri, D. Z. Yankelevsky, and O. Rabinovitch, 2020, "Blast response of one-way arching masonry walls," *International Journal of Impact Engineering* 141(3): 1–16, DOI: 10.1016/j.ijimpeng.2020.103568.

[7] X. Zhou, A. S. Ackerman, A. M. Fridlind, R. Wood, and P. Kollias, "Impacts of solar-absorbing aerosol layers on the transition of stratocumulus to trade cumulus clouds," *Atmospheric Chemistry and Physics*, 17(20): 12725–12742, Oct. 2017, DOI: 10.5194/ACP-17-12725-2017.

[8] M. Keshava and S. R. Raghunath, 2017 "Experimental Investigations on Axially and Eccentrically Loaded Masonry Walls," *Journal of The Institution of Engineers (India): Series A*, 98(4): 449–459 DOI: 10.1007/S40030-017-0222-2/METRICS.

[9] M. S. Dharek, S. Raghunath, and C. P. Ashwin, 2021 "Experimental behaviour of unreinforced and reinforced concrete block masonry walls under uniaxial compression," Materials Today: Proceedings, 46: 2462–2467. DOI: 10.1016/J.MATPR.2021.01.398.

[10] M. S. Dharek, P. Sunagar, K. Harish, K. S. Sreekeshava, S. U. Naveen, and Bhanutej, 2020. "Performance of Self-flowing Concrete Incorporated with Alumina Silicates Subjected to Elevated Temperature," L*ecture Notes in Civil Engineering* 74: 111–120, DOI: 10.1007/978-981-15-4079-0_10/COVER.

[11] C. Pettit, E. Mohsin, C. Cruz-Noguez, and A. Elwi, 2021 "Experimental testing of slender load-bearing masonry walls with realistic support conditions," *Canadian Journal of Civil Engineering* 49(1): 95–108, DOI: 10.1139/CJCE-2020-0297.

[12] Vindhyashree, Alfa Rahamath, Dr. Prema Kumar W. P., and Dr. Prathap Kumar M. T., 2015, "Numerical Simulation of Masonry Prism Test using ANSYS and ABAQUS," *IJERT – International Journal of Engineering Research & Technology,* 4(07): 1019–1027, DOI: 10.17577/ijertv4is070814.

[13] P. B. Lourenço, 1996. "Computational strategies for masonry structures," Delft University, Netherlands, [Online]. Available: http://www.narcis.nl/publication/RecordID/oai:tudelft.nl:uuid:4f5a2c6c-d5b7-4043-9d06-8c0b7b9f1f6f

[14] J. H. Doh and S. Fragomeni, 2015 "Evaluation of Experimental Work on Concrete Walls in One and Two-Way Action," *Australian Journal of Structural Engineering* 6(1): 37–52, DOI: 10.1080/13287982.2005.11464943.

[15] J. H. Doh, S. Fragomeni, and J. W. Kim, 2001. "Brief Review of Studies on Concrete Wall Panels in One and Two Way Action," *International Journal of Ocean Engineering and Technology* 4(1): 38-43 https://www.researchgate.net/publication/29455344_Brief_Review_of_Studies_on_Concrete_Wall_Panels_in_One_and_Two_Way_Action (accessed Dec. 18, 2022).

[16] C. Busse, A. P. Kach, and S. M. Wagner, "Boundary Conditions: What They Are, How to Explore Them, Why We Need Them, and When to Consider Them," *Organizational Research Methods,* 20(4): 574–609, Oct. 2017, DOI: 10.1177/1094428116641191.

[17] O. A. Kamal, G. A. Hamdy, and T. S. El-Salakawy, 2014. "Nonlinear analysis of historic and contemporary vaulted masonry assemblages," *HBRC Journal* 10(3): 235–246. DOI: 10.1016/j.hbrcj.2013.11.004.

[18] M. Hasan, T. Saidi, D. Sarana, and Bunyamin, 2021 "The strength of hollow concrete block walls, reinforced hollow concrete block beams, and columns," *Journal of King Saud University – Engineering Sciences*., DOI: 10.1016/J.JKSUES.2021.01.008.

[19] A. Oan, … N. S. 12th N. A. M. C., and undefined 2015, "The effect of horizontal reinforcement embedded in bond beams in concrete masonry walls," Res. Oan, NG Shrive Proceedings of the 12th North American Masonry Conference (12NAMC) Denver, Colorado, •researchgate.net, 2015, Accessed: Aug. 16, 2023. [Online]. Available: https://www.researchgate.net/profile/Ahmed-oan/publication/330858132_the_effect_of_horizontal_reinforcement_embedded_in_bond_beams_in_concrete_masonry_walls/links/5c58cea1299bf12be3fcf083/the-effect-of-horizontal-reinforcement-embedded-in-bond-beams-in-concrete-masonry-walls.pdf

[20] S. Iffat, 2015, "Relation Between Density and Compressive Strength of Hardened Concrete,"*Concrete Research Letters*. 6(4), Accessed: Aug. 16, 2023. [Online]. Available: www.crl.issres.net

[21] Y. H. Mugahed Amran, A. A. Abang Ali, R. S. M. Rashid, F. Hejazi, and N. A. Safiee, 2016. "Structural behavior of axially loaded precast foamed concrete sandwich panels," *Construction and Building Materials*. 107: 307–320, DOI: 10.1016/J.CONBUILDMAT.2016.01.020.

[22] M. Pavanetto, L. Sbrogiò, M. Salvalaggio, and M. R. Valluzzi, 2020, "Equivalent frame modelling of an unreinforced masonry building in finite element environment," *Lecture Notes in Mechanical Engineering* 2006–2021, DOI: 10.1007/978-3-030-41057-5_160/COVER.

[23] T. Choudhury, G. Milani, and H. B. Kaushik, 2020, "Experimental and numerical analyses of unreinforced masonry wall components and building," *Construction and Building Materials.* 257: 119599, DOI: 10.1016/J.CONBUILDMAT.2020.119599.

[24] X. Zhou and B. Feng, 2023, "A smeared-crack-based field-enriched finite element method for simulating cracking in quasi-brittle materials," *Theoretical and Applied Fracture Mechanics*, 124: 103817, DOI: 10.1016/J.TAFMEC.2023.103817.

[25] E. V. Caburnay, L. M. Danao, and E. D. Magdaluyo, 2023, "Finite Element Analysis of an External Fixator with Composite Connecting Rods," in *Lecture Notes in Engineering and Computer Science*, 2245: 124–128.

[26] S. Serin Main, C. Author, M. Ahmet Oğuzhanoğlu, and C. Kayadelen, 2021 "Comparative analysis of stress distributions and displacements in rigid and flexible pavements via finite element method", *Revista de la Construcción. Journal of Construction.* 20(2) DOI: 10.7764/RDLC.20.2.321.

[27] A. Eslami, H. R. Ronagh, S. S. Mahini, and R. Morshed, 2012 "Experimental investigation and nonlinear FE analysis of historical masonry buildings - A case study," *Construction and Building Materials*., 35: 251–260, DOI: 10.1016/j.conbuildmat.2012.04.002.

[28] ANSYS, 1989. "Structural analysis software," *International Journal of Fatigue* 11(3): 199–199, DOI: 10.1016/0142-1123(89)90443-x.

[29] T. El-Salakawy and G. Hamdy. 2021, "Experimental and numerical investigation of strengthening of openings in masonry walls using steel bars and steel wire mesh," *European Journal of Environmental and Civil Engineering* 1–19. DOI: 10.1080/19648189.2021.1997828.

[30] S. C. Ganapathi et al. 2009, "Experimental and numerical study of confined masonry walls under in-plane loads : case : guerrero State (Mexico)," *European Journal of Environmental and Civil Engineering,* 11(1): 62–73, DOI: 10.1504/IJSTRUCTE.2021.112103. (active DOI?)

[31] M. Z. Kalali, A., & Kabir, 2010. "Modelling of unreinforced brick walls under in-plane shear and compression loading.," *Structural Engineering and Mechanics* 36(3): 247–278,

[32] T. pradeep Selvakumar Viswanathan, Sinthiya Ravi1 and V. S. and P. N. Nagarajan1, 2014 "Numerical Simulation of Compression and Shear Behaviour of Unreinforced Brick Masonry," *International Conference on Biological, Civil and Environmental Engineering (BCEE-2014) March 17-18, 2014 Dubai (UAE).*

[33] N. Sathiparan and U. Rumeshkumar, 2018, "Effect of moisture condition on mechanical behavior of low strength brick masonry," *Journal of Building Engineering*. 17: 23–31, DOI: 10.1016/J.JOBE.2018.01.015.

[34] B. Yang, 2005, "Stress Analysis in Two-Dimensional Problems," in Stress, Strain, and Structural Dynamics, Elsevier, 135–156. DOI: 10.1016/b978-012787767-9/50006-4.

[35] A. Elamin and H. Lei, 2020 "The Fatigue Failure Analysis of Steel Structure and Review of Collapse Accidents," *International Journal of Advanced Engineering Research and Science (IJAERS)*. 7(7): 314–323, DOI: 10.22161/ijaers.77.35.

[36] M. Yang, Y. Akiyama, and T. Sasaki, 2004, "Evaluation of change in material properties due to plastic deformation," *Journal of Materials Processing Technology* 151(1–3): 232–236. DOI: 10.1016/J.JMATPROTEC.2004.04.114.

[37] P. Hawi and R. Ghanem, 2024, "Mesh Refinement As Probabilistic Learning," *Journal of Machine Learning for Modeling and Computing* 5(4): 1–21, DOI: 10.1615/JMACHLEARNMODELCOMPUT.2024054830.

[38] S. I. Fundi, J. W. Kaluli, and J. Kinuthia, 2018, "Performance of interlocking laterite soil block walls under static loading, *Construction and Building Materials* 171: 75–82, DOI: 10.1016/J.CONBUILDMAT.2018.03115.